Accepted for publication. DOI: 10.1109/WPT.2017.7953857

Conjugate Image Theory for Non-Symmetric Inductive, Capacitive and Mixed Coupling

Ben Minnaert* and Nobby Stevens*, *Member, IEEE*
*Department of Electrical Engineering, KU Leuven, Technology Campus Ghent, Ghent, Belgium
Email: ben.minnaert@kuleuven.be

***Abstract*—The conjugate image theory provides a methodology to determine the optimal circuit for a given wireless link. In this work, we compare the application of this theory between inductive and capacitive wireless power transfer, extended to non-symmetric configurations. We apply the conjugate image theory for mixed coupling and demonstrate that the results for inductive and capacitive coupling can be deduced from this configuration. Our results enable the description of the optimal circuit network of both an inductive and a capacitive system in compact equations, valid for the series and parallel topology. This allows a better understanding of the fundamental properties of the wireless transfer link, essential for efficient power transfer.**

Keywords: wireless power transfer, inductive coupling, capacitive coupling, mixed coupling, impedance matching.

I. Introduction

Fig. 1 shows the most basic example of an inductive wireless link, capable of wirelessly transferring energy from a time harmonic voltage source V_S to a load R_{sL}. It consists of two coupled coils L_1 and L_2 with mutual inductance L_M. The magnetic coupling factor k_L of the link is defined as:

$$k_L = \frac{L_M}{\sqrt{L_1 L_2}} \tag{1}$$

The efficiency of power transfer can be significantly increased by creating resonant circuits. This can be realized by adding capacitances C_{s1} and C_{s2} at the transmitter and receiver side. The power transfer efficiency is also influenced by the value of the load R_{sL} [1], [2]. Since any reactance of the load can be included into the series capacitance C_{s2}, we limit ourselves to purely resistive loads.

From the conjugate image theory, the optimal values for these capacitances and load that realize the maximum power transfer efficiency can be calculated for a given wireless link and working angular frequency ω [3], [4]. These optimal values are well-known and described in detail in literature, e.g., [1], [5]–[7]. The conjugate image theory can also be applied on capacitive coupling to determine the optimal load and compensation elements [8], [9]. However, a rigorous comparison of the application of the conjugate image theory for inductive (IPT) and capacitive (CPT) power transfer is not yet published. In this work, we perform a compact comparison for non-symmetric configurations. Moreover, we apply the conjugate image theory for mixed coupling and illustrate that the results for IPT and CPT can be deduced from the mixed configuration. This work extends previous work [9] to non-symmetric systems.

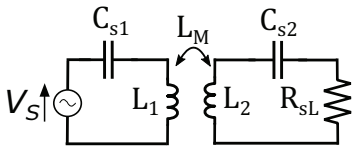

Fig. 1. Equivalent circuit of an inductive wireless power transfer system from a time harmonic voltage source V_S to a load R_{sL}, consisting of two coupled coils L_1 and L_2 with mutual inductance L_M and compensation elements C_{s1} and C_{s2}.

II. Methodology

A. Inductive coupling

The wireless inductive link of Fig. 1 can be characterized as a two-port network with impedance matrix $\mathbf{Z} = \mathbf{R} + j\mathbf{X}$, with elements $z_{ij} = r_{ij} + jx_{ij}$ $(i, j = 1, 2)$, given by:

$$z_{11} = j\omega L_1 \tag{2}$$

$$z_{12} = z_{21} = j\omega L_M \tag{3}$$

$$z_{22} = j\omega L_2 \tag{4}$$

Given the impedance matrix $\mathbf{Z}$, the conjugate image theory allows the straightforward calculation of the optimal values for the series capacitances C_{s1} and C_{s2}, and the optimal load R_{sL} [3]:

$$R_{sL} = r_{22}\sqrt{1 - \frac{r_{12}^2}{r_{11}r_{22}}}\sqrt{1 + \frac{x_{12}^2}{r_{11}r_{22}}} \tag{5}$$

$$X_1 = \frac{r_{12}x_{12}}{r_{22}} - x_{11} \tag{6}$$

$$X_2 = \frac{r_{12}x_{12}}{r_{11}} - x_{22} \tag{7}$$

with X_i the reactance of the capacitor C_{si} defined as

$$X_{Ci} = -\frac{1}{\omega C_{si}} \tag{8}$$

We find:

$$R_{sL} = \omega L_M \tag{9}$$

$$C_{si} = \frac{1}{\omega^2 L_i} \tag{10}$$

We impose that the series and parallel topology of Fig. 2 are equivalent, i.e., both circuits have the same impedance. This

978-1-5090-4585-3/17/$31.00 ©2017 IEEE

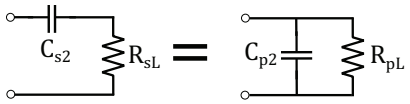

Fig. 2. We define C_{p2} and R_{pL} by imposing that the series and parallel network are equivalent.

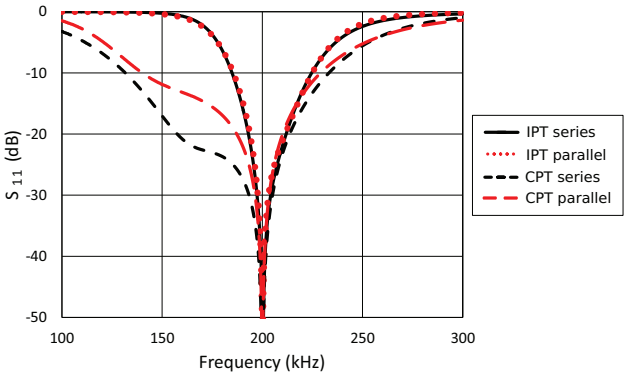

Fig. 3. The S_{11} parameter as function of frequency for an IPT and CPT system, optimized for 200 kHz, for the series and parallel topology.

implies the definition of C_{p2} and R_{pL}, and taken into account (9) and (10), we obtain:

$$R_{pL} = \frac{\omega(L_2^2 + L_M^2)}{L_M} \tag{11}$$

$$C_{p2} = \frac{L_2}{\omega^2(L_2^2 + L_M^2)} \tag{12}$$

Equation (10) corresponds with the expression found in [4]. However (9), (11) and (12) differ from the results by Inagaki [4] since our expressions are also valid for non-symmetrical inductive coupling.

To numerically validate the above analytical derivation, we simulate in SPICE an IPT system with $L_1 = 20$ μH, $L_2 = 30$ μH and $L_M = 6$ μH. For a working frequency of 200 kHz, we find from (9) and (10) an optimal load of $R_{sL} = 7.54$ Ω with series capacitances $C_{s1} = 31.7$ nF and $C_{s2} = 21.1$ nF. We simulate the S_{11} and S_{21} parameter for this circuit with the above values and a voltage source with internal resistance equal to the load. Fig. 3 and Fig. 4 confirm the validity of (9) and (10), indicated by the minimum and maximum of S_{11} and S_{21}, respectively, at the working frequency of 200 kHz. The same conclusions can be drawn for the parallel topology: from (11) and (12), we find an optimal parallel load of $R_{pL} = 196$ Ω and parallel capacitance $C_{p2} = 20.3$ nF at 200 kHz. We obtain similar results (Fig. 3 and Fig. 4).

B. Capacitive coupling

Wireless power transfer can also be realized by capacitive coupling. The equivalent circuit of capacitive coupling (Fig. 5) consists of two coupled capacitances C_1 and C_2 with mutual capacitance C_M [9], [10]. The electric coupling factor k_C of the link is defined as:

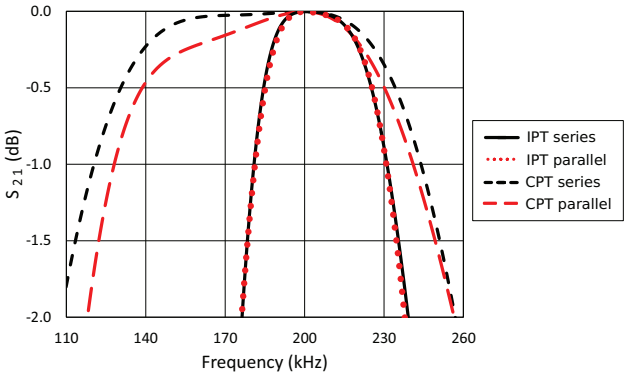

Fig. 4. The S_{21} parameter as function of frequency for an IPT and CPT system, optimized for 200 kHz, for the series and parallel topology.

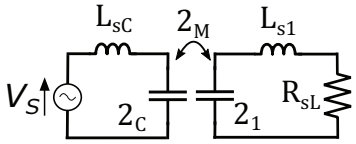

Fig. 5. Equivalent circuit of a capacitive wireless power transfer system from a time harmonic voltage source V_S to a load R_{sL}, consisting of two coupled capacitances C_1 and C_2 with mutual capacitance C_M and compensation elements L_{s1} and L_{s2}.

$$k_C = \frac{C_M}{\sqrt{C_1 C_2}} \tag{13}$$

For ease of notation, we define $\gamma_C = C_1 C_2 - C_M^2$. The impedance matrix elements of this wireless link are given by:

$$z_{11} = \frac{C_2}{j\omega\gamma_C} \tag{14}$$

$$z_{12} = z_{21} = \frac{C_M}{j\omega\gamma_C} \tag{15}$$

$$z_{22} = \frac{C_1}{j\omega\gamma_C} \tag{16}$$

Resonance is obtained by introducing inductors in series or parallel. Following analogous notation and methodology as for inductive coupling, and with the definition of the reactance X_L of the inductor

$$X_{Li} = \omega L_i \tag{17}$$

we obtain, with $(i, j) = (1, 2)$ or $(2, 1)$:

$$R_{sL} = \frac{C_M}{\omega\gamma_C} \tag{18}$$

$$L_{si} = \frac{C_j}{\omega^2\gamma_C}, \tag{19}$$

$$R_{pL} = \frac{C_1^2 + C_M^2}{\omega C_M \gamma_C} \tag{20}$$

TABLE I
DEFINITION OF L' FOR IPT AND C' FOR CPT FOR THE DIFFERENT CONFIGURATIONS, WITH $(i,j) = (1,2)$ OR $(2,1)$.

	L' (IPT)	C' (CPT)
R_{sL}	L_M	$\frac{\gamma_C}{C_M}$
X_{si}	L_i	$\frac{\gamma_C}{C_j}$
R_{pL}	$\frac{L_2^2+L_M^2}{L_M}$	$\frac{\gamma_C C_M}{C_1^2+C_M^2}$
X_{p2}	$\frac{L_2^2+L_M^2}{L_2}$	$\frac{\gamma_C C_1}{C_1^2+C_M^2}$

$$L_{p2} = \frac{C_1^2 + C_M^2}{\omega^2 C_1 \gamma_C} \tag{21}$$

Equation (19) corresponds with earlier results [9] where (18), (20) and (21) differ since they are also valid for non-symmetrical inductive coupling.

Notice that for as well IPT as CPT, we considered a lossless approximation of a real wireless link, i.e. any resistances of the wireless link are neglected. It was experimentally demonstrated [4], [9] that this assumption is acceptable for this application.

We simulate in SPICE a CPT system with $C_1 = 200$ nF, $C_2 = 150$ nF, $C_M = 100$ nF. For a working frequency of 200 kHz, we find from (18) and (19) an optimal load of $R_{sL} = 3.98\ \Omega$ with series inductances $L_{s1} = 4.75\ \mu$H and $L_{s2} = 6.33\ \mu$H. For the parallel topology, we calculate from (20) and (21) an optimal parallel load of $R_{pL} = 19.9\ \Omega$ with an optimal parallel inductance of $L_{p2} = 7.92\ \mu$H. The results, shown in Fig. 3 and Fig. 4, confirm the analytical derivation.

C. Comparison

If we define an inductor L' for IPT and capacitor C' for CPT, given by Table I, we can elegantly write the optimal load R_L for maximum power transfer efficiency, either in series or parallel topology, as the reactance of L' or C':

$$R_L = \begin{cases} X_{L'} & \text{for IPT} \\ -X_{C'} & \text{for CPT} \end{cases} \tag{22}$$

The optimal compensation elements for IPT and CPT can also be expressed as the reactance of L' or C', as defined in Table I:

$$\begin{cases} X_{Ci} = -X_{L'} & \text{for IPT} \\ X_{Li} = -X_{C'} & \text{for CPT} \end{cases} \tag{23}$$

With the above compact expressions, we can determine the optimal load and compensation elements for both inductive and capacitive wireless power transfer, for as well series as parallel topology.

III. MIXED COUPLING

We now use the conjugate image theory to determine the optimal compensation elements and load for a mixed coupling configuration where both inductive and capacitive coupling are present. We will show that the separate cases of inductive and capacitive coupling can be deduced as a special case of mixed coupling. Resonance for mixed coupling has applications in e.g., design of microwave bandpass filters and microstrip resonators [11], [12].

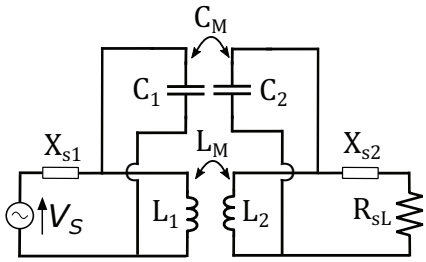

Fig. 6. Equivalent circuit of mixed coupling, consisting of inductive and capacitive coupling in parallel, with reactances X_{s1} and X_{s2} as compensation elements.

Basic mixed coupling can be represented by the network of Fig. 6. The compensation elements X_{s1} and X_{s2} correspond to an inductor and capacitor for positive and negative reactances, respectively. Since mixed coupling is the parallel configuration of an inductive and capacitive coupling, we can easily determine the admittance matrix $\mathbf{Y}$ of the two port system by summing the admittance matrices for capacitive and inductive coupling. For ease of notation, we define $\gamma_L = L_1 L_2 - L_M^2$. The matrix elements y_{ij} $(i,j = 1,2)$ of $\mathbf{Y}$ for this configuration are given by [12]:

$$y_{11} = j\omega C_1 + \frac{L_2}{j\omega\gamma_L} \tag{24}$$

$$y_{12} = y_{21} = j\omega C_M - \frac{L_M}{j\omega\gamma_L} \tag{25}$$

$$y_{22} = j\omega C_2 + \frac{L_1}{j\omega\gamma_L} \tag{26}$$

The impedance matrix $\mathbf{Z}$ is then given by

$$[Z] = \frac{1}{D_Y}\begin{bmatrix} y_{22} & -y_{12} \\ -y_{21} & y_{11} \end{bmatrix} \tag{27}$$

with D_Y the determinant of the admittance matrix $\mathbf{Y}$:

$$D_Y = -\omega^2\gamma_C - \frac{1}{\omega^2\gamma_L} + \frac{1}{\gamma_L}(L_1C_1 + L_2C_2 - 2L_MC_M) \tag{28}$$

From (5), (6) and (7), we find

$$R_s = -\frac{1}{D_Y}(\omega C_M + \frac{L_M}{\omega\gamma_L}) \tag{29}$$

$$X_{si} = -\frac{1}{D_Y}(\omega C_j - \frac{L_i}{\omega\gamma_L}) \tag{30}$$

$$R_{pL} = -\frac{(\omega^2 C_M\gamma_L + L_M)^2 + (\omega^2 C_1\gamma_L - L_2)^2}{D_Y\omega\gamma_L(\omega^2 C_M\gamma_L + L_M)} \tag{31}$$

$$X_{p2} = -\frac{(\omega^2 C_M \gamma_L + L_M)^2 + (\omega^2 C_1 \gamma_L - L_2)^2}{D_Y \omega \gamma_L (\omega^2 C_1 \gamma_L - L_2)} \quad (32)$$

A positive and negative reactance corresponds to an inductor and capacitor, respectively.

If we reduce the circuit of Fig. 6 to the inductive circuit of Fig. 1 by posing C_1=C_2=C_M=0 in the above four expressions, the expressions reduce to (9), (10), (11) and (12), i.e., the expressions for inductive coupling. If we reduce the circuit to the capacitive circuit of Fig. 5 by posing L_1=L_2=∞ and L_M=0, the expressions reduce to (18), (19), (20) and (21), i.e., the expressions for capacitive coupling.

IV. Conclusion

We introduced a generic comparison for the application of the conjugate image theory on non-symmetric inductive and capacitive wireless power transfer, valid for both the series and the parallel topology. Implementation of this theory on mixed coupling demonstrates that inductive and capacitive coupling can be considered as a special case of this configuration.

Acknowledgment

This work was executed within MoniCow, a research project bringing together academic researchers and industry partners. The MoniCow project was co-financed by imec (iMinds) and received project support from Flanders Innovation & Entrepreneurship.

References

[1] M. Dionigi, M. Mongiardo and R. Perfetti, "Rigorous network and full-wave electromagnetic modeling of wireless power transfer links", *IEEE Trans. Microw. Theory Techn.*, 63(1), pp. 65-75, 2015.

[2] B. Minnaert and N. Stevens, "Single variable expressions for the efficiency of a reciprocal power transfer system", *Int. J. Circ. Theor. App.*, 2016.

[3] S. Roberts, "Conjugate-image impedances", *Proc. of the IRE*, 34(4), pp. 198p-204p, 1946.

[4] N. Inagaki, "Theory of image impedance matching for inductively coupled power transfer systems", *IEEE Trans. Microw. Theory Techn.*, 62(4), pp. 901-908, 2014.

[5] G. Monti, A. Costanzo, F. Mastri and M. Mongiardo, "Optimal design of a wireless power transfer link using parallel and series resonators", *Wirel. Power Transf.*, 3, pp. 105-116, 2016.

[6] A. Costanzo, M. Dionigi, D. Masotti, M. Mongiardo, G. Monti, L. Tarricone and R. Sorrentino, "Electromagnetic energy harvesting and wireless power transmission: A unified approach", *Proc. IEEE*, 102, pp. 1692-1711, 2014.

[7] K. Aditya, M. Youssef and S.S. Williamson, "Analysis of series-parallel resonant inductive coupling circuit using the two-port network theory", *Proc. of the IEEE IECON*, Yokohama, Japan, pp. 5402-5407, Nov. 2015.

[8] M. Dionigi, M. Mongiardo, G. Monti and R. Perfetti, "Modelling of wireless power transfer links based on capacitive coupling", *Int. J. Numer. Model.*, 2016.

[9] B. Minnaert and N. Stevens, "Conjugate Image Theory Applied on Capacitive Wireless Power Transfer", *Energies*, 10(1), 46, 2017.

[10] L. Huang and A.P. Hu, "Defining the mutual coupling of capacitive power transfer for wireless power transfer", *Electron. Lett.*, 51(22), pp. 1806-1807, 2015.

[11] V.V. Tyurnev, "Coupling coefficients of resonators in microwave filter theory", *Prog. Electromagn. Res. B.*, 21, pp.47-67, 2010.

[12] J.S. Hong and M.J. Lancaster, "Couplings of microstrip square open-loop resonators for cross-coupled planar microwave filters", *IEEE Trans. Microw. Theory Techn.*, 44(11), pp.2099-2109, 1996.